Simulations of a Shaped Dielectric Lens Antenna by FEKO

Y. Tajima and [1]Y. Yamada

Department of Electrical and Electronic Engineering, National Defense Academy
1-10-20 Hashirimizu, Yokosuka-shi, 239-8686 JAPAN
[1] yyamada@nda.ac.jp

Abstract – In the Intelligent Transportation System (ITS), millimeter waves are used and antennas are requested to have beam scanning ability. In the millimeter wave operation, a dielectric lens antenna is one of the prominent candidates. Authors designed a shaped dielectric lens antenna based on the Abbe's sine condition. Wide angle beam scanning characteristics were ensured through the ray tracing calculations and radiation pattern measurement. Recently, owing to the enhancement of electromagnetic simulator abilities, simulations of a dielectric lens antenna become possible. By employing an electromagnetic simulation, it is expected that detailed electrical performances of both the feed horn and the dielectric lens will be made clear. In this paper, electromagnetic simulations of a shaped dielectric lens antenna by FEKO suit 5.3 are conducted. First, the corrugate horn used for the feed horn is electromagnetically simulated. Excellent simulated radiation patterns coinciding with the measured results are achieved. Next, the feed horn radiation patterns are combined with the dielectric lens simulations. And simulation results of beam scanning characteristics are obtained. When comparing the simulated scanned beam shapes with the measured results, very good agreements are obtained. So, accuracies of simulations are ensured. Moreover, unexpected sidelobe increases in the specific wide angle region that were pointed out previously are studied. Simulated and measured results can confirm the sidelobe increases. As an additional study, electrical field distributions in the dielectric lens are simulated. Then, multiple reflections between lens surfaces are visually made clear. The reason of sidelobe increases can be clearly understood. As a result, it is confirmed that the FEKO simulator can rigorously simulate electromagnetic characteristics of a shaped dielectric lens antenna.

Keywords: Dielectric Lens Antenna, Wide Angle Beam Scanning and Wide Angle Radiation Pattern.

I. INTRODUCTION

In the Intelligent Transportation System (ITS), millimeter waves are used and antennas are requested to have beam scanning ability in the collision avoidance system. Here a dielectric lens antenna is one of the prominent candidates which achieves wide angle beam scanning [1]. Authors designed and fabricated the shaped dielectric lens antenna [2]. The wide angle radiation patterns were examined through ray tracing calculations [3] and measurements [4]. Good agreements of calculated and measured results were ensured. However, in the case of the ray tracing method, the electric performance of the feed horn was approximated by a simple mathematical function. For more exact analysis, FDTD method is used for calculation of lens antennas. However it requires huge computer memory and calculation time [5]. In order to reduce calculation memory, axi-symmetrical FDTD is developed [6]. Even though the method can reduce calculation memory, it can not calculate off-focus feed. And Method of Moment (MoM) can be also used for calculation of homogeneous dielectric body [7]. In this method, instead of a volume distribution, calculation can be formulated in terms of a surface distribution and calculation memory can be reduced. And an electromagnetic simulation ability handling a dielectric lens antenna is enhanced in the FEKO suit 5.3 based on MoM. By employing this electromagnetic simulator, both the feed horn and the dielectric lens antenna can be analyzed exactly.

In this paper, FEKO calculation results of detailed electrical characteristics on the corrugate horn used as the feed horn and the shaped dielectric lens antenna are obtained. And radiation patterns are compared with the measured results in order to ensure the calculation accuracies. In section 2, the outline of the shaped dielectric lens antenna is explained. And summaries of simulation parameters and computer loads are explained. In section 3, simulation conditions of the corrugate horn so as to coincide with the measured results are shown. In section 4, simulated and measured results of beam scanning characteristics on the shaped lens antenna are shown. In section 5, as for wide angle radiation patterns, simulated and measured results are shown. Remarkable sidelobe increases in the specific wide angle region are indicated. In order to clarify the reason, electrical fields in the lens are investigated and trials of matching layers attachment on the lens surfaces are conducted.

II. SHAPED DIELECTRIC LENS ANTENNA FOR WIDE ANGLE BEAM SCANNING

A. Configuration of The Lens Antenna

Figure 1 shows the configuration of the shaped dielectric lens antenna in the simulation and the measurement. The lens has axi-symmetrical structure around the Z-axis. A corrugate horn is employed as the feed horn. And the lens and the feed are surrounded by an electromagnetic absorber in order to suppress spill over. The lens material is Teflon and surfaces are designed by introducing Abbe's sine condition [8]. The focal length L_f of 105mm and the lens diameter D of 100mm are employed. The frequency of 60GHz (λ=5mm) are employed. The lens diameter is corresponding to 20λ. The beam scan is achieved by off focus feed shown as a broken line and the off-focus position of 25° scanning beam (θ_s=25°) is indicated. At the time, the length between the horn and the lens center L_f' becomes 81.9mm. The polarizations of the feed horn are also shown. The electrical field component of the horn is parallel to the Y-axis. For the off-focus position, the coordinate system is rotated around the Y-axis. The new axis are denoted by the X' and Z' as shown in the figure. And the plane on which the horn moves (ZX-plane) is called as a scanning plane and the plane which transverse the scanning plane (YZ or YZ'-plane) is called as the transverse plane.

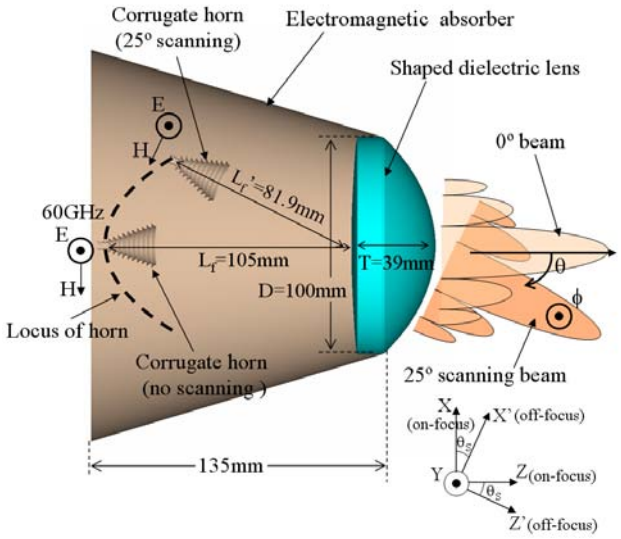

Fig. 1. Lens antenna configuration.

The specification of a personal computer and simulation parameters are shown in Table 1. In calculation, the FEKO simulator that can use the Multilevel Fast Multipole Method (MLFMM) is employed in order to save the computer memory and speed up to calculation time. Surface Equivalence Principle (SEP) and Volume Equivalence Principle (VEP) are employed for the calculation of the dielectric lens and electromagnetic absorber, respectively. So, all antenna parts can be simulated by the Method of Moment. The mesh size of λ/8 is employed for the corrugate horn. For the dielectric lens and electromagnetic absorber, mesh size of λ/3 is employed because these dielectric objects are very large compare to one wave length. The mesh size might look too coarse, there is a little difference in radiation pattern shapes and null depths in mesh size of λ/3 to λ/7. So, the dielectric objects of mesh size of λ/3 can be simulated accurately. As for the dielectric constant of the electromagnetic absorber, the catalog data of ε_r=2 and tanδ=1 is used. The dielectric lens and the electromagnetic absorber require large memory of 2.6GByte and 3.1GByte respectively. The calculation time is 44.4 hours and it corresponds to about 2 days.

Table 1. Simulation parameters.

Computer specification	CPU	Xeon 3.2GHz
	Loaded memory (Byte)	20G
	Software	FEKO (Suit 5.3), MOM with MLFMM
Feed horn (Corrugate horn)	Mesh size	λ/8
	Number of mesh	13,102
	Calculation memory (Byte)	365M
Dielectric lens	ε_r	1.94
	Tanδ	7.5×10^{-4}
	Mesh size	λ/3
	Number of mesh	33,843
	Calculation Memory (Byte)	2.6G
Electromagnetic absorber	ε_r	2
	tanδ	1
	Thickness	10mm
	Mesh size	λ/3
	Number of mesh	75.346
	Calculation Memory (Byte)	3.1G
Calculation time (h)	44.4	

B. Estimation of Beam Scanning by a Ray Tracing Method

Outlines of the beam scanning abilities can be anticipated through the ray tracing results. Rays from the feed horn to the lens outside are calculated by the ray tracing software developed by authors. Rays emitted from the positions of θ_s=0° and 25° are shown in Figs. 2(a) and (b), respectively. In Fig. 2(a), rays in the X-axis and the Y-axis directions become parallel after refraction by the shaped dielectric lens. From results of the rays, an axi-symmetrical pencil beam is expected. In Fig. 2(b), while rays in the X-axis direction become parallel after refraction by the lens, rays in the Y-axis direction do not

become parallel. Moreover, rays do not exist in a flat plane and compose a curved plane. So, phase deterioration in the Y-axis direction is suspected. Also, it is suspected that the beam shape will be distorted in the transverse plane.

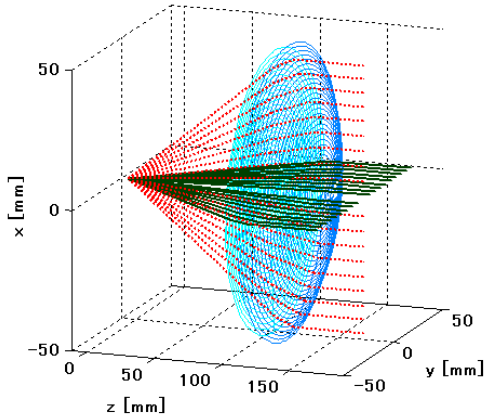

(a) No scanning

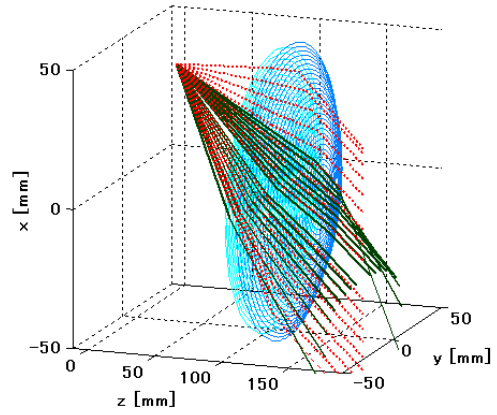

(b) 25° scanning

Fig. 2. Rays on the scanning and transverse directions.

III. SIMULATION CONDITIONS OF THE FEED CORRUGATE HORN

The corrugated horn used in the simulation is designed depending on the measured horn structure shown in Fig. 3. The simulated horn is excited at the feed point by an electric point source, while the actual horn is connected with a wave guide. The depth of the groove is optimized in order to achieve the scalar feed characteristics and to coincide with the measured radiation patterns. At the distant points on the lens surface, the phase center of the corrugate horn becomes 20mm inside from the aperture.

Figure 4 shows simulated and measured radiation patterns. The simulated patterns are shown by dotted lines and the measured patterns are shown by solid lines. As a result of the scalar feed, the patterns of E and H-plane become almost the same. As a result of adequate horn parameters, the radiation patterns of simulated and measured results agree very well. The 3dB beam width of each pattern is 21°. Edge levels of the lens antenna become -15 dB and -18 dB at θ_s = 0° and θ_s = 25°, respectively.

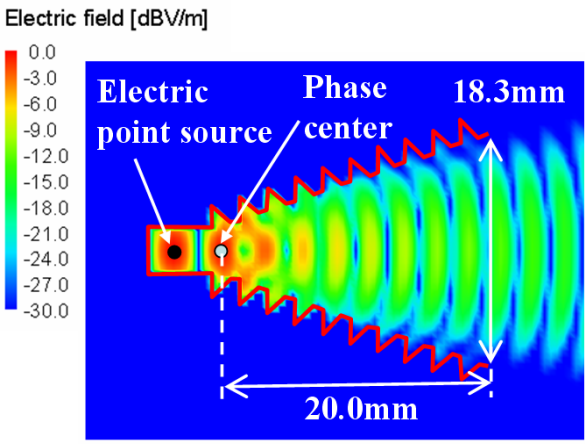

Fig. 3. Corrugate feed horn.

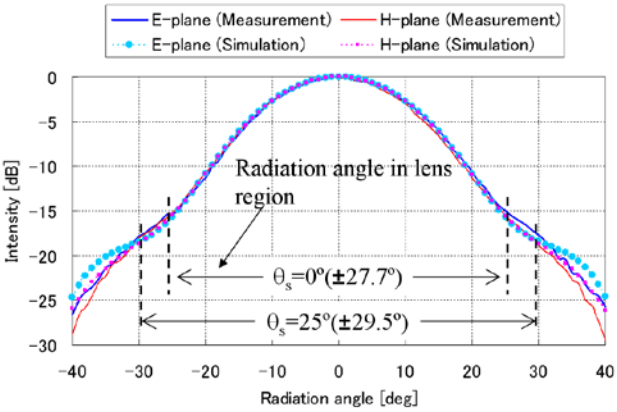

Fig. 4. Radiation patterns of the corrugate feed horn.

IV. BEAM SCANNING CHARACTERISTICS

Figure 5 shows a photograph in measurements of the lens antenna. The lens is supported by a plastic plate covered by an electromagnetic absorber. The feed horn is supported by the positioning mount. The positioning mount can be moved along the X and Z-axis and rotated around the Y-axis. In the measurement setting, the far filed criterion given by $2(d_1+d_2)^2/\lambda$ is 6.2m and the range between the lens antenna and a receiving antenna is 4.4m. So, adequate radiation patterns can be obtained.

A. No Scanning Beam Pattern

Measured and simulated radiation patterns of on focus feed are shown in Fig. 6. The simulated patterns are

shown by broken lines and the measured patterns are shown by solid lines. In Figs. 6(a) and (b), the radiation patterns on the scanning and transverse planes become almost same due to the scalar feed characteristics of the feed horn. Beam widths on the scanning and transverse planes are 3.6° and 3.5°, respectively. As for comparisons of the measured and the simulated patterns, very good agreements are achieved. In the case, the lens material (Teflon) permittivity of 1.96 is employed. So, 1.96 is suitable for the permittivity of Teflon at the frequency of 60GHz. The antenna gains of measurement and simulation are 34.7dBi and 34.2dBi, respectively. These antenna gains agree very well. The simulated gain is 1.8dB lower than the uniformly illuminated aperture gain of 36.0dBi. This gain reduction corresponds to the aperture efficiency of 66%. Loss factors of the lens antenna are summarized in Table 2. Total loss of 2.2dB agrees well to the simulated gain reduction of 1.8dB.

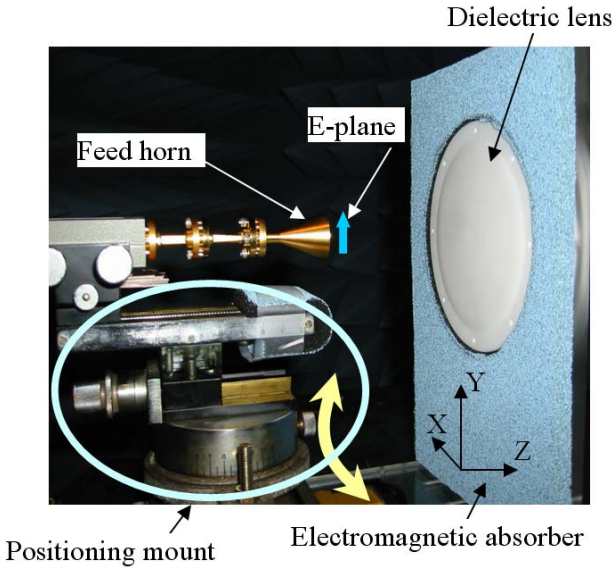

Fig. 5. Measurement setting.

Table 2. Loss factors.

	Gain	Loss
Uniform illumination	36.0dBi	
Intensity taper		0.74dB
Reflection		0.25dB
Dielectric loss		0.13dB
Spill over		1.12dB
Total loss		2.24dB
Calculated gain	33.8dBi	
Simulated gain by FEKO	34.2dBi	1.8dB

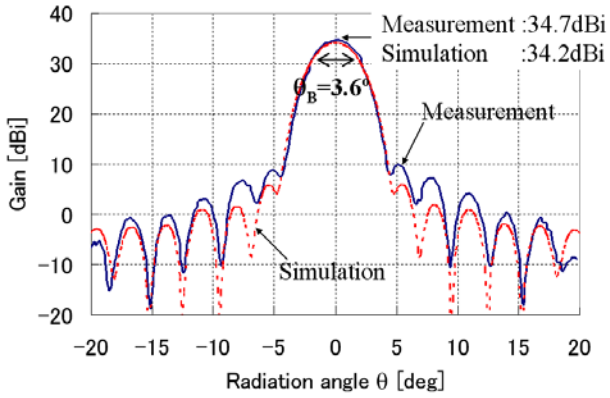

(a) Scanning-plane (H-plane)

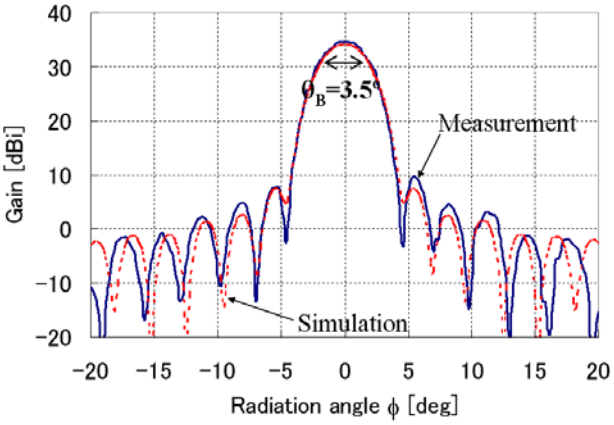

(b) Transverse-plane (E-Plane)

Fig. 6. Radiation patterns of lens antenna (no scanning).

B. 25° Scanning Beam Pattern

Measured and simulated radiation patterns in the case of 25° scanning are shown in Figs. 7(a) and (b). The measured and the simulated patterns agree well. The measured and simulated 3dB beam widths in the scanning-plane are 4.0°. And at radiation angle of 15°<θ<20°, shoulder patterns are observed in both of the measurement and simulation. It indicates that the small phase error is occurred on the plane. In the transverse-plane, 3dB beam widths of measurement and simulation become 5.4°. And the main lobes deteriorate to broaden shapes. Comparing with the no scanning beam, the scanning-plane beam width is broadened only 0.4°. However the transverse-plane beam width is broadened about 1.9°. The reason of this beam broadening is considered that phase deviation is produced in the transverse-plane. The gains of measurement and simulation are 32.1dBi and 31.8dBi, respectively. These gain reductions are corresponding to the beam widths broaden.

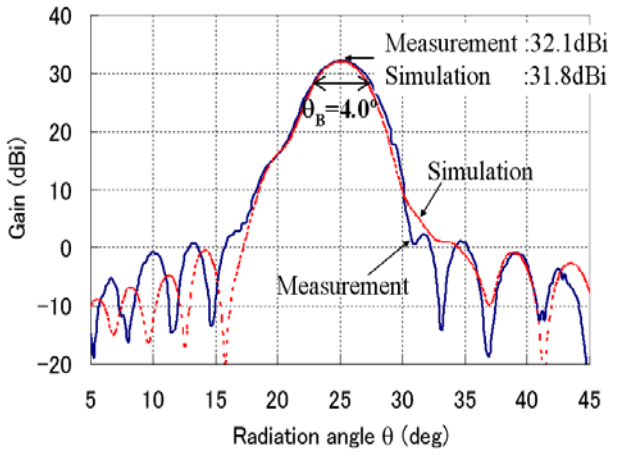

(a) XZ-plane (Scanning)

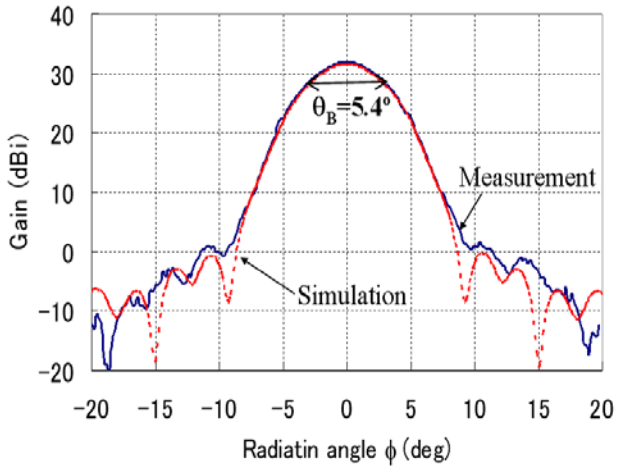

(b) YZ-plane (Transverse)

Fig. 7. Radiation patterns of lens antenna (25° scanning).

In order to understand the reason of beam broadening, the field intensity and phase distributions on the X'Y-plane of the lens aperture are shown in Figs. 8(a) and (b). In the field intensity, almost axi-symmetrical pattern is obtained as shown in Fig. 8(a). This distribution is almost satisfactory. In Fig. 8(b), the phase distribution along the scanning direction is almost constant due to the lens surface shaping. However, the phase distribution along the transverse direction is delayed to the aperture edge and the difference between the center and the edge is more than 150°. This large phase delay is considered the cause of the transverse-plane radiation deterioration. In order to correct the phase delay, array antenna configuration to the feed is effective [9].

As conclusions of beam scanning characteristics, calculation results by the FEKO simulator agree very well with measured results. So, calculation accuracies are ensured.

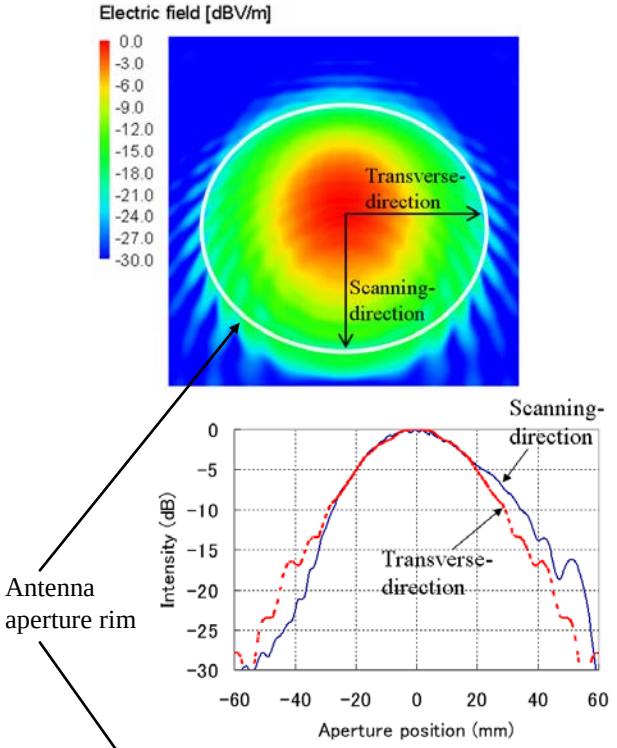

(a) Field intensity (X'Y-plane).

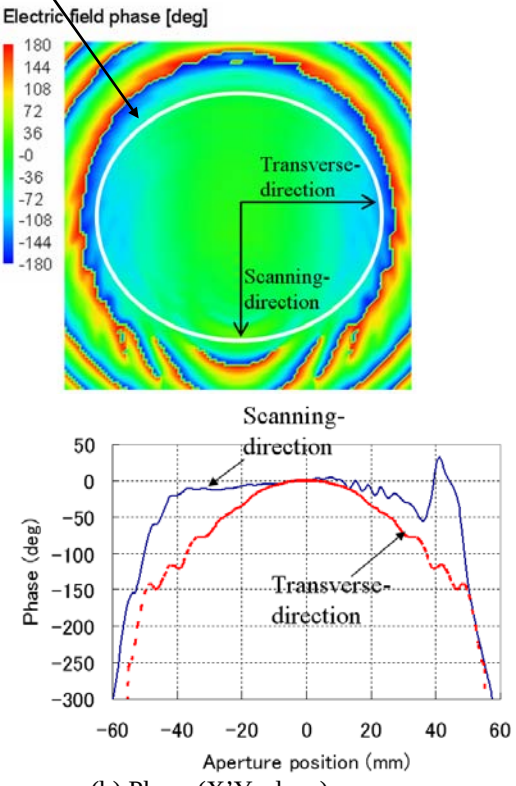

(b) Phase (X'Y-plane).

Fig. 8. Aperture electrical field distributions.

V. WIDE ANGLE RADIATION PATTERN

Previously, it was reported that multi-reflections between lens surfaces increased radiation levels in specific wide angle region [4]. So, we tried to clarify the multiple reflections through electromagnetic simulations. Figure 9 shows measurement setting of wide angle radiation pattern. In the case of measurement, the feed horn and lens edge are covered by the electromagnetic absorber.

Measured and calculated radiation patterns in the wide angle region are shown in Fig. 10. In the measured result, almost symmetrical pattern is obtained. So, the measurement accuracy is ensured. Sidelobe levels are decreasing gradually to 40 degree. However, sidelobe levels suddenly increase at 45°. Sidelobe levels become almost -10dBi in the angle region 45°<|θ|<75°. Measured and simulation patterns agree very well. Both the simulation and measurement results indicate sidelobe increases precisely. So, simulations of this phenomenon are considered accurate.

In order to investigate the reason of sidelobe increase, electric field in the lens is shown in Fig. 11. Inside the dielectric lens, many high intensity lines are observed. Judging from the directions of lines, these lines indicate reflections from the front surface. Outside the front surface, weak radiations to wide angle regions are observed and these radiations are thought the cause of the sidelobe increase. Next in order to investigate surface reflections precisely, ray tracing results are obtained by the ray tracing software developed by authors. Ray tracing results are shown in Fig. 12. The incoming rays to the lens antenna are shown by dotted lines. Reflected rays are shown by solid lines. First, incoming rays are reflected at the front surface. Then, reflected rays are once again reflected at the rear surface. Finally, dually reflected rays are radiated in wide angle regions. Through the electromagnetic simulations and the ray tracing calculations, the reason of sidelobe increases in the wide angle region is clarified.

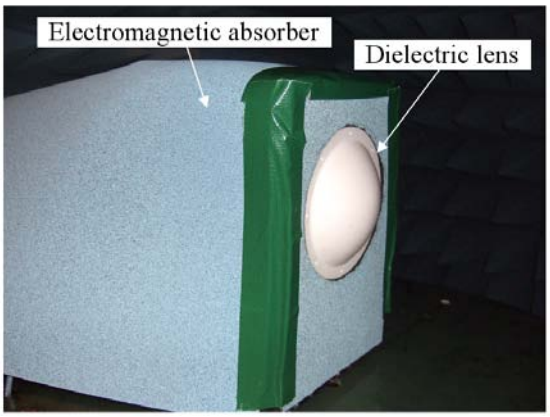

Fig. 9. Measurement setting of wide angle radiation pattern.

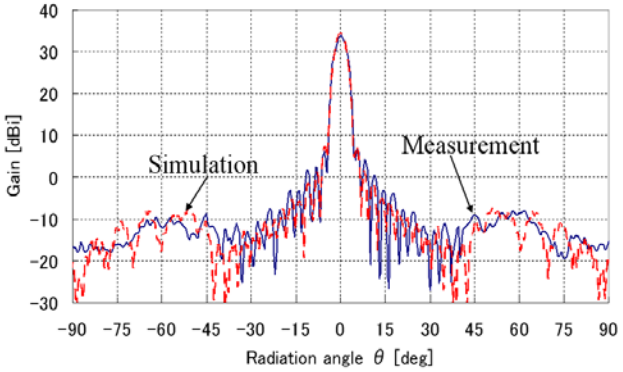

Fig. 10. Wide angle radiation pattern (without matching layer).

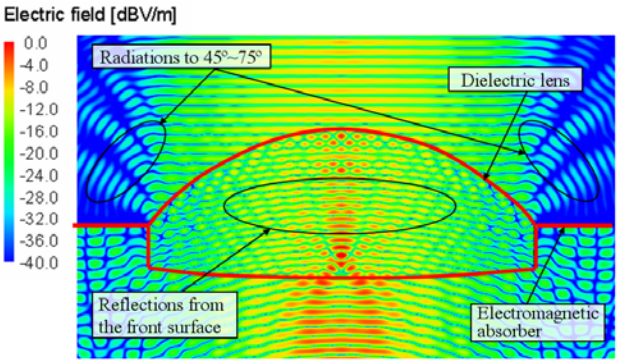

Fig. 11. Electric fields in the lens.

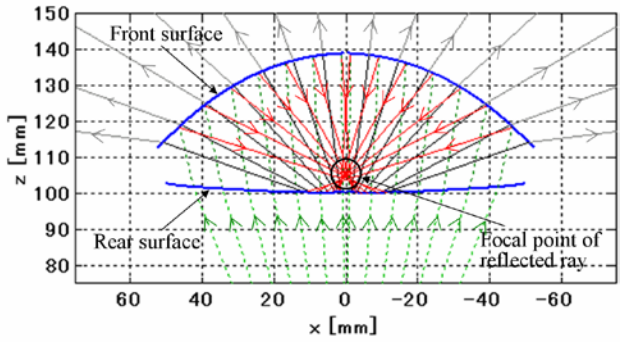

Fig. 12. Ray trace of multiple reflections.

One more trial to ensure multiple reflections is conducted by attaching matching layers on the lens surfaces. Situations of matching layers are shown in Fig. 13. The material of matching layers is foamed Teflon. Its permittivity is assumed as 1.41 and its thickness is 1.0mm ($\approx\lambda_g/4$). The matching layers are attached on the dielectric lens with double-stick tape.

The measured and simulation results are shown in Fig. 14. In the measured and simulated results, increased sidelobes in the angle region 45°<|θ|<75° are sufficiently suppressed. However, because the matching layers are not

completely designed, small sidelobe increases remain in the angular region 60°<|θ|<90° in the simulation and 40°<|θ|<90° in the measurement, respectively. Next in order to understand the effect of matching layers, electrical fields in the lens are obtained. Simulated results are shown in Fig. 15. Reflected waves from the front surface become very weak. The effects of matching layers are ensured. In designing matching layers, the ray tracing results of Fig. 12 provide the very important data. Reflected rays from the front surface concentrate in front of the rear surface. So, the designed matching conditions carefully at the center region of the rear surface seems the most important.

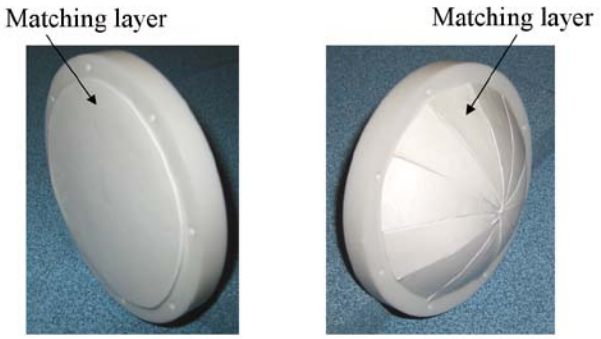

(a) Rear surface (Feed side) (b) Front surface (Aperture side)

Fig. 13. Matching layer.

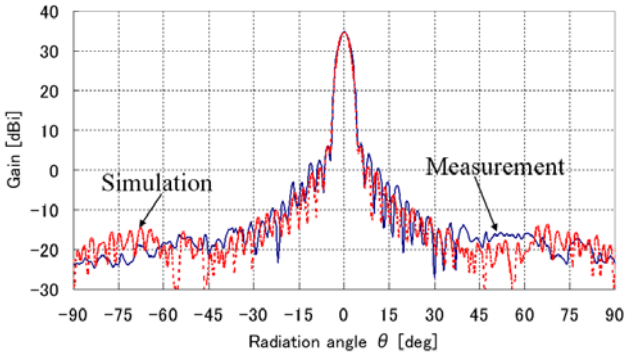

Fig. 14. Wide angle radiation pattern (with matching layer)

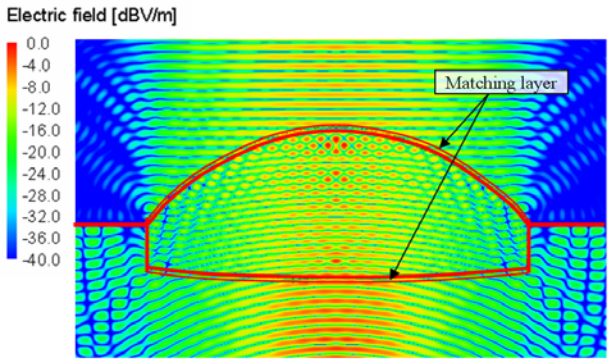

Fig. 15. Electric fields in the lens.

As conclusions of simulations of wide angle radiation characteristics, it is ensured that FEKO simulator can produce exact electromagnetic solutions. Moreover, very interesting phenomena of multiple reflections between lens surfaces are visually clarified.

VI. CONCLUSIONS

In accordance with the improvement of simulation abilities for dielectric objects in FEKO suit 5.3, authors tried to simulate the shaped dielectric lens antenna developed by authors. Accuracies of simulations are ensured through comparing the simulated results with measured results. Moreover, some interesting phenomena happened in the lens are visually clarified.

- Beam scanning characteristics that are the main subject of the shaped dielectric lens antenna could be simulated successfully. Simulation accuracies are ensured through the good agreement with the measured results.
- Amplitude and phase distributions of electrical fields on the antenna aperture plane are visually clarified in the case of beam scanning.
- Affects on radiation patterns of multiple reflections inside the lens are exactly simulated and simulated radiation patterns agree very well with the measured results.
- Electrical field distributions indicating multiple reflections inside the lens are shown and this phenomenon are visually clarified.

ACKNOWLEDGEMENT

Authors express thanks to Dr. Naobumi Michishita of National Defense Academy for his helpful discussions.

REFERENCES

[1] T. Kato et. al., “76 GHz high performance rader sensor featuring fine step scanning mechanism utilizing NRD technology,” *IEEE Intelligent Vehicles Symposium*, pp. 163-170, May 2001.

[2] Y. Tajima and Y. Yamada, “Design of shaped dielectric lens antennas for wide angle beam steering”, *WILEY Periodicals Inc., Electron. and Comm. in Japan*, Part 3, vol. 89, no. 2, pp. 1-12, Feb. 2006.

[3] Y. Tajima, Y. Yamada, S. Sasaki, and A. Kezuka, “Calculation of wide angle radiation patterns and caustics of a dielectric lens antenna by a Ray tracing method”, *IEICE Trans.*, vol. E-87-C, no. 9, pp. 1432-1440, Sep. 2004.

[4] Y. Tajima, Y. Yamada, and A. Kezuka, “Measured results of dielectric lens antenna for wide angle bean scanning”, *IEICE Trans. in Japanese*, vol. J88-B, no. 12, pp. 2394-2397, Dec. 2005.

[5] A. Kezuka, Y. Yamada, and H. Kida, "Radiation pattern syntheseis of a lens horn antenna", *IEICE Trans.*, vol. E87-C, no. 9, pp. 1425-1431, Sep. 2004.
[6] A. Kezuka, Y. Yamada, and Y. Kazama, "Phase correction method for GO designed dielectric lens horn antenna", *IEICE Trans.*, vol. E88-B, no. 6, pp. 2334-2340, June 2005.
[7] R. F. Harrington, *Field Computaion by Moment Methods*, *IEEE PRESS*, pp. 38-40, 1993.
[8] Y. T. Lo and S. W. Lee, *Antenna Handbook*, volume 2, Van Nostrand Reinhold Company, Ch. 16, pp. 16-23, 1988.
[9] Y. Tajima and Y. Yamada, "Improvement of beam scanning characteristics of a dielectric lens antenna by array feeds", *IEICE Trans*., vol. J91-A no. 7, pp. 1616-1624, Jun. 2008.

Tajima was born in Oita, Japan on February 28, 1978. He received the B.S. and M.S. degrees in Electronics Engineering from National Defense Academy, Kanagawa, in 2000 and 2005. He enlisted in Japan-Air-Self-Defense-Force in 2000. He was engaged in tests and developments of radar equipments. Now he is a Capt. He entered the doctor course of Electronics and Information Engineering of National Defense Academy. His current research interests include lens antennas and array antennas.

Yoshihide Yamada graduated from Nagoya Institute of Technology and received the BS and MS degrees of electronics in 1971 and 1973, respectively. And he received the DE degree from Tokyo Institute of Technology in 1989. In 1973 he joined the Electrical Communication Laboratories of Nippon Telegraph and Telephone Corporation (NTT). Till 1984, he was engaged in research and development of reflector antennas for terrestrial and satellite communications. From 1985, he engaged in R&D of base station antennas for mobile radio systems. In 1993, he moved to NTT Mobile Communications Network Inc. (NTT DoCoMo). In 1995, he was temporarily transferred to YRP Mobile Telecommunications Key Technology Research Laboratories Co., Ltd. At the same time, he was a guest professor of the cooperative research center of Niigata University, and a lecturer of Science University of Tokyo, both from 1996. In 1998, he changed his occupation to a professor of National Defense Academy. Now, he is interested in very small RFID antennas, shaped dielectric lens antennas and electromagnetic simulations of large objects. He is a member of the IEICE and JSST of Japan and IEEE society members of AP, VT and COMM.